A Novel FcγR-Defined, IgG-Containing Organelle in Placental Endothelium[1]

Toshihiro Takizawa,[2]* Clark L. Anderson,† and John M. Robinson[3]*

Placental transfer of IgG from maternal circulation to that of the fetus is crucial for fetal and newborn immunity. This process requires that IgG broach two cellular layers of the placenta. IgG transport across the first layer, the syncytiotrophoblast, is almost certainly mediated by the MHC-related FcR for IgG, FcRn. The second layer, the villus endothelium, was until recently thought to allow IgG movement nonspecifically by constitutive transcytosis in caveolae. However, we recently showed that villus endothelium expressed a separate FcR for IgG, the inhibitory motif-bearing FcγRIIb2 seen most notably on macrophages and as a minor fraction of the FcγRIIb expressed on B cells. Now, by quantitative microscopy, we find FcγRIIb2 to be expressed abundantly in an unidentifiable and likely novel organelle of the villus endothelium, unassociated with caveolae. About half of these FcγRIIb2 organelles contain IgG; the remainder lack IgG. The majority fraction (~80%) of IgG-containing organelles is associated with FcγRIIb. No IgG-containing organelles are associated with caveolin. These findings are compatible with FcγRIIb-mediated transfer of IgG across the villus endothelium, independent of caveolae. *The Journal of Immunology,* **2005, 175: 2331–2339.**

The human placenta transports IgG from maternal circulation to the circulation of the fetus conferring a full complement of protective maternal Abs to the neonate for the first few months of life while its own immune system matures. This mechanism, not yet clearly defined, requires IgG movement across two cell layers of the placenta, the syncytiotrophoblast (STB)[4] and the endothelium. Almost certainly, transport across the former is mediated by FcRn, which is the MHC-related FcR for IgG (reviewed in Refs. 1 and 2). This receptor expresses high affinity for IgG at low pH but no affinity at physiologic pH, so an efficient transcytotic mechanism moving IgG from acidic vesicles to the basolateral surface of the cell, although not yet thoroughly substantiated, can readily be envisioned. How IgG traverses the endothelium is considerably less clear. It has been presumed that transfer occurs passively in transcytosing caveolae (reviewed in Ref. 3).

Complicating this tidy view is the recent observation that another FcR, FcγRIIb2, is expressed in placental endothelium. Expression is abundant in the terminal villus but diminishes down the vascular tree to the cord in which no FcγRIIb2 is seen or expressed as is the case in any other endothelium of the adult body (4). Yet FcγRIIb2 appears on several cells of the immune system where it is found in varying ratios with its better-studied isoform, FcγRIIb1 (recently discussed in Refs. 4–6). The two isoforms are distinguished solely by a 19 amino acid insert (47 amino acids in mouse) in the cytoplasmic tail of FcγRIIb1, encoded by an extra exon. The cytoplasmic tails of both isoforms feature a characteristic amino acid motif centered on a phosphorylated tyrosine (ITIM) that attracts Src homology 2 domain-containing enzymes and adaptor molecules. According to studies performed mostly with the FcγRIIb1 isoform, a variety of inhibitory responses thus emanate from this motif. Because both isoforms bear the motif, it is inferred that both are capable of antagonizing cellular functions. In the mouse these two isoforms have been shown to be functionally distinctive, FcγRIIb2 mediating endocytosis and transcytosis via clathrin-coated pits and vesicles, whereas FcγRIIb1, because of the cytoplasmic insert, is somehow excluded from the endocytic mechanism (7–9).

What function FcγRIIb2 might perform at this endothelial site is unknown. Two hypotheses have been proposed: 1) that it transports IgG across the cell, most likely in caveolae, and 2) that it moves immune complexes to lysosomes for degradation (10, 11). We report a series of quantitative microscopy studies designed to probe how IgG moves across the endothelium. Testing the conjecture that IgG moves in caveolae, we find that caveolin (CAV) does not colocalize in the same subcellular compartment with IgG, suggesting indeed, that caveolae are not transcytosing IgG. Rather, we find that the great majority (80%) of intracellular IgG is associated with the FcγRIIb compartment. Roughly half of the FcγRIIb organelles contain IgG; the other half is devoid of IgG. Further, we show that the FcγRIIb-expressing organelle is the most abundant membrane-bounded compartment in these cells and would appear novel and previously unidentified.

Materials and Methods

Reagents

The primary Abs used in this study are described in Table I. Alexa 488- and 594-labeled secondary Abs, Alexa 488-labeled anti-human IgG, 4′,6′-diamidino-2-phenylindole (DAPI), and the ProLong anti-photobleaching kit were from Molecular Probes. HRP- or FITC-tagged secondary Abs

*Department of Physiology and Cell Biology and †Department of Internal Medicine, Ohio State University, Columbus, OH 43210

Received for publication December 21, 2004. Accepted for publication May 27, 2005.

The costs of publication of this article were defrayed in part by the payment of page charges. This article must therefore be hereby marked *advertisement* in accordance with 18 U.S.C. Section 1734 solely to indicate this fact.

[1] This work was supported in part by the National Institutes of Health Grants HD38764 (to J.M.R.) and CA88053 (to C.L.A.).

[2] Current address: Department of Molecular Anatomy, Nippon Medical School, 1-1-5 Sendagi, Bunkyo-ku, Tokyo 113-8602, Japan.

[3] Address correspondence and reprint requests to Dr. John M. Robinson, Department of Physiology and Cell Biology, Ohio State University, 304 Hamilton Hall, 1645 Neil Avenue, Columbus, OH 43210. E-mail address: robinson.21@osu.edu

[4] Abbreviations used in this paper: STB, syncytiotrophoblast; DAPI, 4′,6-diamidino-2-phenylindole; IFM, immunofluorescence microscopy; CAV, caveolin; EEA 1, early endosome Ag 1; LAMP, lysosome-associated membrane protein; IEM, immunoelectron microscopy; EM, electron microscopy; NHDF, normal human dermal fibroblast; DIC, differential interference contrast; ECM, extracellular matrix.

Copyright © 2005 by The American Association of Immunologists, Inc.

0022-1767/05/$02.00

Table I. *Primary Abs used in this study*

Abs	Species	Marker Protein	Source	Reference
CAV-1 (clone 2297)	Mouse	Caveolae	BD Transduction Laboratories	12
CAV-2 (clone 65)	"	Caveolae	"	13
Clathrin H chain	"	Coated pits	"	14
EEA 1	"	Early endosomes	"	15
Bip/GRP	"	Endoplasmic reticulum	"	16
GM130	"	Golgi matrix	"	17
p230	"	*Trans*-Golgi network	"	18
Cathepsin D	"	Lysosomes	"	19
LAMP 1	"	Late endosomes/lysosomes	Developmental Studies Hybridoma Bank	20
LAMP 2	"	Late endosomes/lysosomes	"	20
M6PR	"	Late endosomes/TGN	Affinity Bioreagents	21
TfR	"	Early and recycling endosomes	Zymed Laboratories	22
CD 31	"	Endothelial plasma membrane	P. Newman[a]	23
FcγRIIb (KB61)	"	FcγRIIb	D. Mason[b]	24
Dynamin II	Rabbit	Coated pits	Santa Cruz Biotechnology	25
Factor VIII related antigen	"	Endothelial Weibel-Palade bodies	Zymed Laboratories	26
FcγRIIb (163.96)	"	FcγRIIb	J. Teillaud[c]	4
FcγRIIa	"	FcγRIIa	J. Frey[d]	4
CAV-1α	Chicken	Caveolae	J. Robinson[e]	27 and 28

[a] P. Newman, Blood Research Institute, Milwaukee, Wisconsin.
[b] D. Mason, Radcliffe Hospital, Oxford, U.K.
[c] J. Teillaud, Institut Curie, Paris, France.
[d] J. Frey, University of Bielefeld, Bielefeld, Germany.
[e] J. Robinson, Ohio State University, Columbus, Ohio.

(donkey anti-rabbit and anti-chicken $F(ab')_2$ and biotin SP-conjugated affinity-purified $F(ab')_2$ donkey anti-human IgG were from Jackson ImmunoResearch Laboratories). Goat anti-HRP 5-nm colloidal gold Ab and goat anti-FITC 10-nm colloidal gold Ab were from BB International. Other chemicals used in this study were the same as we have used previously (29).

Tissue processing to obtain ultrathin cryosections

Human full-term placentas were obtained according to a protocol approved by the Ohio State University Human Subjects Institutional Review Board. Tissue samples from uncomplicated Cesarean deliveries were processed for fixation as soon as possible following delivery (within 20 min) as we described (29). Ten placentas were used in this study.

After 4% paraformaldehyde fixation, the tissue was dissected to collect terminal and intermediate villi. These villi, in washing buffer (200 μl), were mixed with 20% gelatin at 37°C (200 μl) and centrifuged in a microfuge (29). Villi in solidified gelatin were processed to prepare ultrathin cryosections as described (30).

High resolution immunofluorescence microscopy (IFM)

IFM assays were conducted on ultrathin cryosections of placental villi as we have described (29). Dilutions for the primary Abs were: caveolin (CAV)-1, CAV-2, early endosome Ag 1 (EEA 1), cathepsin D, and p230 (5 μg/ml); clathrin H chain, GM130, Bip, and transferrin receptor (10 μg/ml); dynamin II (4 μg/ml); mannose-6-phosphate receptor (20 μg/ml); lysosome-associated membrane protein (LAMP) 1 (4.9 μg/ml); LAMP 2 (4.1 μg/ml); CD31 (6.9 μg/ml); KB61 (culture supernatant 1/2 dilution); factor VIII related antigen (1/50 dilution); chicken CAV-1α (1/500 dilution); FcγRIIa (260) (1/100 dilution); FcγRIIb (163.96) (1/3200 dilution). With CAV-1 and CAV-2, an Ag retrieval procedure was used (27).

The Alexa-labeled secondary Abs were diluted 1/200. Alexa-labeled anti-human IgG was diluted 1/100. Controls consisted of replacing the primary Ab with normal serum or by omitting the primary Ab. Nuclei were stained with DAPI for 10 min, then washed five times in PBS, and coverslips were mounted on slides in ProLong.

Immunoelectron microscopy (IEM)

In IEM, ultrathin cryosections were collected on electron microscopy (EM) grids as we have reported (30). Sections were incubated for the localization of a subset of the Ags (FcγRIIb, CAV-1α, and IgG) in single- or double-labeled preparations. Following immunolabeling, sections were stained with a new positive contrast technique (30). Controls consisted of replacing the primary Ab with normal serum or by omitting the primary Ab.

Cell culture

Normal human dermal fibroblasts (NHDF) and HUVEC were obtained from Cambrex Bioscience. HUVEC were grown in endothelial growth medium 2 and NHDF were grown in fibroblast growth medium 2, the media were from Cambrex.

Cell and tissue lysis

HUVEC and NHDF were removed from culture dishes by trypsinization and washed in growth medium and in PBS. Cell pellets were lysed, for 30 min at 4°C, as we have described (31). Placental samples were enriched in terminal villi and lysed in the same manner as the cells except for being sonicated (three times for 15 s) (28). Protein concentration was determined with the bicinchoninic acid protein assay kit (Pierce).

Ab validation

The usefulness of the primary Abs was validated by immunoblotting lysates to determine whether the protein of interest was expressed in placenta and the Ab recognized a single band of the appropriate m.w. Proteins were separated by SDS-PAGE, transferred to nitrocellulose membranes, and probed with primary and secondary Abs as we have described (28). The second phase of Ab testing consisted of IFM on NHDF or HUVEC using methods routine in our laboratory (27). Each Ab was evaluated on whether it localized to the expected structure in these test samples. Thus to be included in this study each Ab had to: 1) be expressed in placenta; 2) yield a single band by immunoblotting; and 3) yield the expected pattern of localization by IFM in cultured cells.

Microscopy

Fluorescence and differential interference contrast (DIC) images were collected with a Nikon Optiphoto microscope and a Photometrics Cool Snap *fx* camera (Roper Scientific) and captured with the MetaMorph image analysis system (Universal Imaging). EM was conducted with a Philips CM-12 operated at 60 kV. Figures were compiled with Photoshop 7 software (Adobe Systems).

Image analysis

The quantitative image analysis procedures were restricted to capillary endothelial cells of terminal villi. In double-label IFM, four images were collected for each area to be analyzed. Images of the distribution of the two Ags, DAPI-stained nuclei, and the ultrathin cryosection were obtained. The latter two images provide the "reference space" so that the IFM signals can be placed in context. The ability to overlay the IFM signals with the reference space allowed us to draw lines demarcating the cell types present in the cryosections.

The colocalization of FcγRIIb with organelle marker proteins was quantified. The fluorescence and DIC images were merged to delineate the endothelial profiles for the fluorescence images. The area within the cells occupied by the fluorescence signal was determined. The degree of colocalization of FcγRIIb and the different marker Ags was determined using

the MetaMorph colocalization function and was expressed as the percentage of colocalization. For each colocalization pair, 1000 FcγRIIb-positive compartments were used in the analysis. The abundance of the FcγRIIb-positive compartments in comparison to other compartments was determined (Table II).

The topological localization of FcγRIIb and CAV-1α in endothelial cells was determined. The distance from the center of a fluorescent structure to the luminal and abluminal cell surface was measured. A total of 1000 FcγRIIb- and CAV-1α-positive structures were used in this analysis.

The relative amounts of IgG present in different locations in terminal and intermediate villi were made from IFM assays. Fluorescence intensity measurements were made for IgG-containing vesicles in the most apical portion of the STB because these vesicles were likely the most recently internalized. Fluorescence intensity measurements were also made for IgG-containing vesicles in endothelium and the extracellular matrix (ECM). A total of 1000 measurements were made for each location.

IEM preparations were subjected to quantitative analysis by counting colloidal particles indicating the localization of specific Ags; different sized colloidal gold particles were used for the detection of different Ags. The degree of colocalization of CAV-1α and FcγRIIb, of CAV-1α and IgG, and FcγRIIb and IgG was determined.

Results

Validation of Ab specificity

We affirmed that all 17 Abs toward cell constituents identified single placental Ags of appropriate m.w. by immunoblotting, and that all gave the predicted localization patterns in IFM preparations of cultured cells. Fig. 1*A* shows a representative example of these data; the remainder are not shown. A single band of ~105–115 kDa is identified from both placenta and HUVEC by immunoblotting with anti-LAMP 1 Ab (Fig. 1*A*, *right panel*), and the same Ab gives a lysosomal and late endosomal pattern upon IFM (Fig. 1*A*, *left panel*), as predicted (20).

Subcellular localization of FcγRIIb

We analyzed the subcellular expression of FcγRIIb in placental villi by IFM and IEM of ultrathin (≤100 nm) cryosections, which are thin enough to render negligible the coincidence (overlap) of overlying organelles. Two Abs directed toward opposite ends of FcγRIIb were used, one specific for the C-terminal cytoplasmic tail (rabbit 163.96) and the other directed toward the N-terminal extracellular portion (mAb KB61). Double-label preparations using both Abs together showed congruence of the two signals (Fig. 1*B*); specifically, 1113 structures labeled with rabbit 163.96 and 1105 labeled with mAb KB61 were counted in the same endothelial cells and were 99.55% congruent. This finding suggested that both Abs were specific and selective for FcγRIIb and that no non-FcγRIIb molecules were being erroneously scored, thus validating their use. FcγRIIb, identified in placenta sections with rabbit 163.96 and mAb KB61 Abs, was expressed exclusively in endothelial cells and apparently not in the STB, macrophages, or stromal cells. That both of these Abs detect exactly the same sites allowed us to use them interchangeably and to carry out other double-label experiments with primary Abs derived from rabbit, mouse, chicken, and goat. An Ab highly selective for FcγRIIa (Ab 260) did not label these endothelial cells (data not shown).

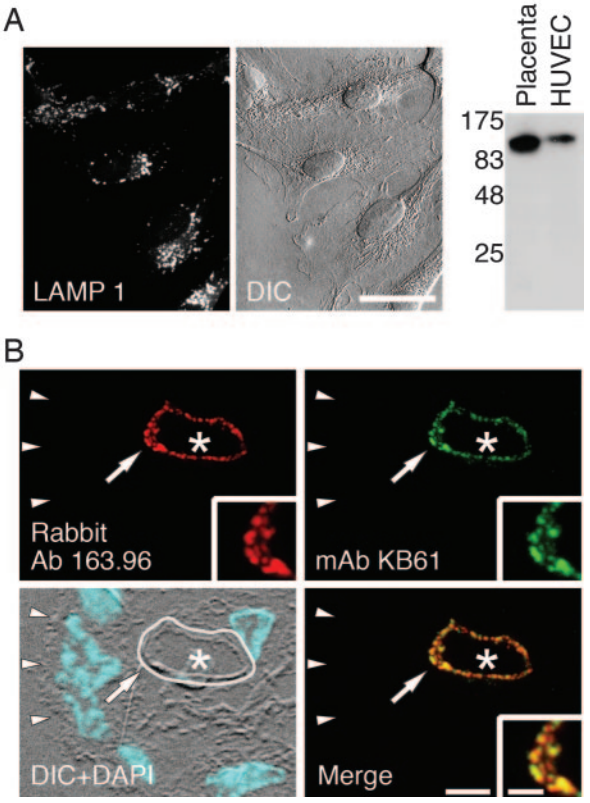

FIGURE 1. The validation of the specificity of Abs. *A*, By IFM anti-LAMP 1 Ab as predicted detects vesicular organelles in the perinuclear region of cultured HUVEC. The companion DIC image shows the morphology of the cells. Bar, 50 μm. An immunoblot of lysates from placenta and HUVEC probed with anti-LAMP 1. Note a single predicted band from both cell and tissue sources. This band was not seen in blots without the anti-LAMP 1 Ab (data not shown). *B*, Double-labeled immunofluorescence localization of FcγRIIb using two different Abs on an ultrathin cryosection of a placental terminal villus. FcγRIIb was localized with a rabbit polyclonal Ab 163.96 (red) and mAb KB61 (green). FcγRIIb was restricted to the capillary endothelium and had the same localization with both Abs. Higher magnification (*inset*) of the region at the arrows is shown. The fluorescence image of DAPI-stained nuclei (*bottom left*, blue) was combined with the DIC image to provide orientation. The red and green fluorescence signals (Merge) show congruency between the two images. Bar, 5 μm; *inset*, 2 μm.

Table II. *Comparison of the abundance of FcγRIIb-positive compartments and compartments containing other marker proteins*[a]

Marker Protein	No. of FcγRIIb-Positive Compartments	No. of Marker Protein-Positive Compartments	Ratio[b]
CAV-1α	5307	5024	1.1
LAMP 1	2545	279	9.1
LAMP 2	4665	412	11.3
EEA 1	3953	277	14.3
p230	4149	32	129.6
GM130	5206	51	102.1

[a] Data derived from double-label IFM assays. The FcγRIIb-positive compartments and marker protein-positive compartments were counted in the same endothelial profiles. In each case, three separate placental preparations were used for counting.

[b] Ratio of FcγRIIb-positive compartments to marker protein-positive compartments.

Novelty of the FcγRIIb organelle

To identify which of the several well-recognized intracellular organelles expressed FcγRIIb we conducted double-label IFM experiments with both anti-FcγRIIb Abs and each of 17 other Abs to marker proteins. The signals for the two markers were scored for overlap. In summation, the FcγRIIb expressing organelle appears novel; it could not be identified as one of the standard intracellular organelles. We illustrated with images of studies with two organelle markers; the remainder gave similar results. First, localization of FcγRIIb to early endosomes was assessed using murine anti-EEA 1 Ab. EEA 1 puncta, abundant in STB, were present in

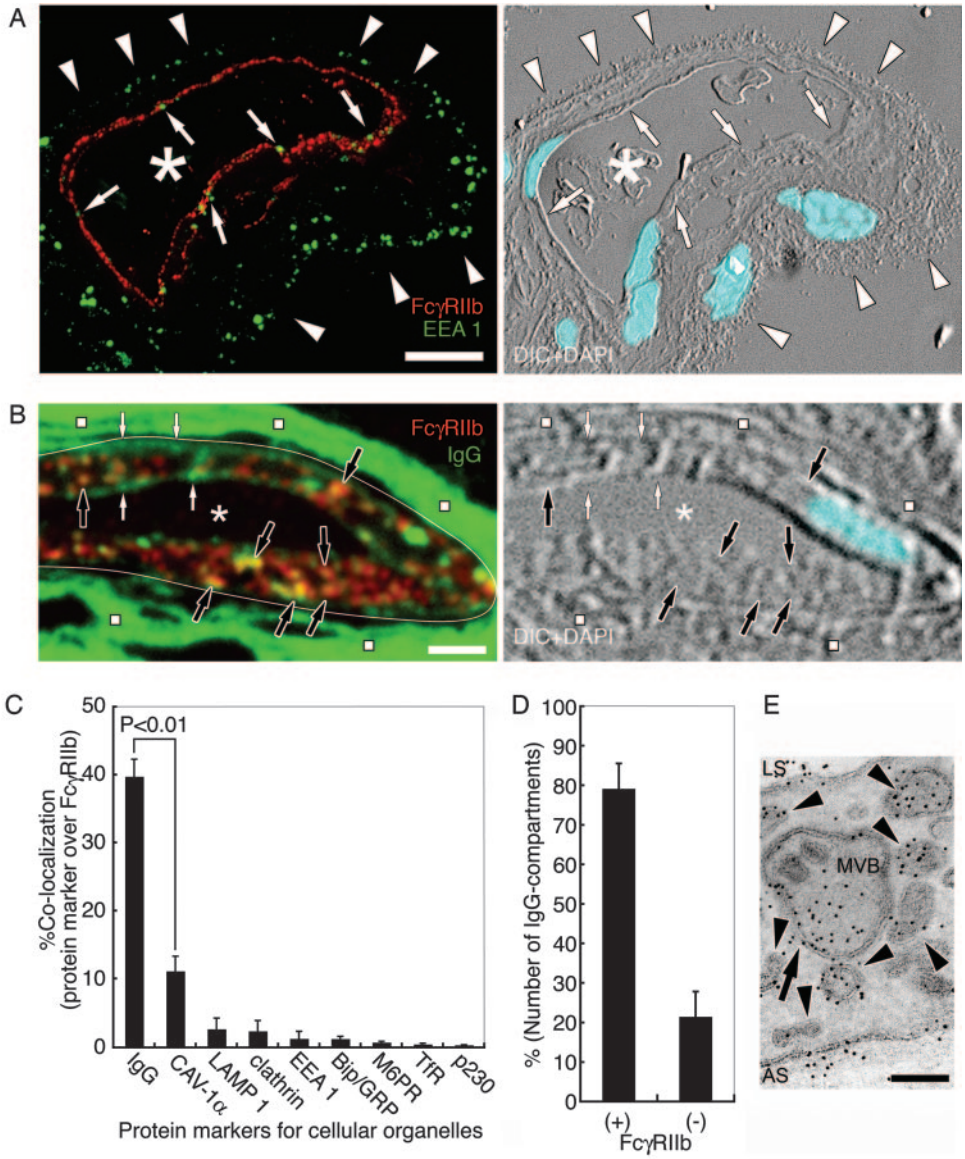

FIGURE 2. FcγRIIb is in a novel organelle. *A*, Double-labeled immunofluorescence localization of FcγRIIb and EEA 1 in an ultrathin cryosection through a placental terminal villus is shown. FcγRIIb (red) was present exclusively in endothelial cells in numerous intracellular structures distributed throughout these cells. The lumen of one capillary is indicated to serve as a landmark (∗). The STB (arrowheads) lacked FcγRIIb. The early endosome marker, EEA 1 (green) was abundant in the STB (arrowheads). EEA 1-positive structures (arrows) while present in endothelial cells were less abundant than were the FcγRIIb-positive structures. The companion DIC image with DAPI-stained nuclei (blue) shows the morphology of the ultrathin section. Bar, 10 μm. *B*, High-resolution double-label immunofluorescence localization of FcγRIIb and human IgG in an ultrathin cryosection of a placental terminal villus. A portion of an endothelial cell (∗, indicates the lumen) and adjacent ECM (white squares) is shown on *left*. The outer boundary of the endothelial cell is indicated with a white line. In the image on the *left* the red and green signals have been merged. FcγRIIb (red) was in vesicular structures in the endothelial cell. IgG (green) was detected in vesicular structures in the endothelium, in association with the luminal and abluminal cell surfaces (white arrows), and in the ECM. There is a significant amount of overlap between the FcγRIIb and IgG signals (black arrows). The companion DIC image (*right*), with DAPI-stained nuclei (blue), shows the morphology of the section. Bar, 2 μm. *C*, FcγRIIb does not colocalize with other organelle marker proteins but does colocalize with IgG. Double-labeled IFM assays in which the localization of FcγRIIb and another organelle marker protein were analyzed using the MetaMorph image analysis software. FcγRIIb colocalized with IgG in ~40% of the FcγRIIb-positive compartments. There was also an apparent low level of colocalization of FcγRIIb with CAV-1α (~10%). None of the other Abs to marker proteins gave colocalization with FcγRIIb that was above background levels. In addition to the marker proteins shown, we also tested for colocalization of FcγRIIb with Abs to GM130, cathepsin D, Factor VIII related antigen, LAMP 2, dynamin II, and CD 31, and none displayed colocalization with FcγRIIb. *D*, Double-label IFM assays for the colocalization of FcγRIIb and IgG were analyzed further. The ~80% of the IgG-containing compartments in capillary endothelial cells contained FcγRIIb signal. *E*, An IEM preparation in which IgG was localized in a capillary endothelial cell using colloidal gold probes is shown. IgG was present in small intracellular vesicular structures (arrowheads). In addition, some IgG was found in larger multivesicular bodies (MVB). This latter localization indicates that a portion of the IgG entering these endothelial cells is destined for degradation. The luminal (LS) and abluminal (AS) sides of the cell are indicated. Bar, 100 nm.

endothelial cells but were sparse compared with FcγRIIb (Fig. 2*A*). The two signals did not overlap (<1%) (Fig. 2*C*). Similar results were noted using murine anti-LAMP 1 and anti-LAMP 2 Abs that recognize marker proteins for late endosomes and lysosomes. LAMP 1- and 2-positive puncta were distributed throughout the STB but were sparse in the endothelium compared with FcγRIIb (data not shown). FcγRIIb-positive structures did not overlap with LAMP 1 or LAMP 2 labeling (Fig. 2*C*).

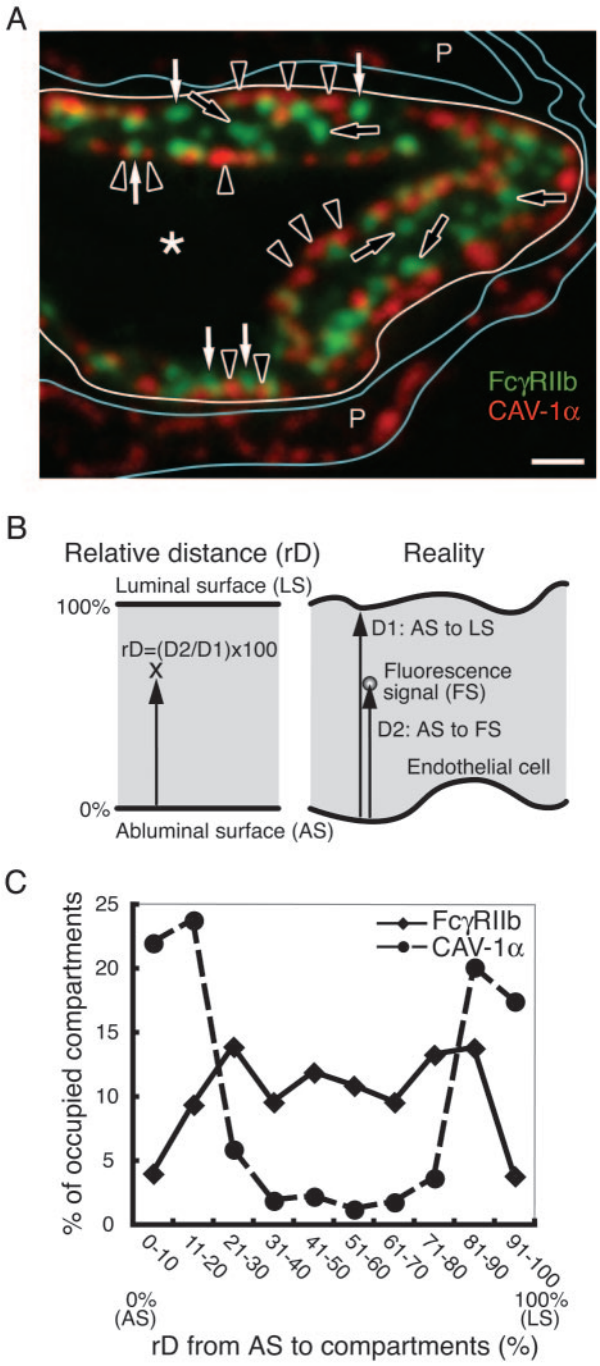

FIGURE 3. The comparison of the distribution of FcγRIIb and CAV-1α in placental endothelial cells. *A*, High-resolution double-label immunofluorescence localization of FcγRIIb and CAV-1α in an ultrathin cryosection through a placental villus. A portion of an endothelial cell (∗, indicates the lumen) and adjacent pericytes (P) are shown. White lines denote the boundaries of the endothelial cell and blue lines show the boundaries of adjacent pericytes. The red and green signals in *A* have been merged. FcγRIIb (green) was localized to vesicular and short tubular structures. Some of the FcγRIIb-positive compartments were located near the cell surface (white arrows), whereas others are located interior to the cell surface (black arrows). CAV-1α (red) was located, almost exclusively, at or just under the cell surface of the endothelial cell (arrowheads). There appeared to be a low level of spatial overlap of the green and red fluorescence signals in the endothelial cells. CAV-1α, but not FcγRIIb, was also localized in the pericytes. Bar, 1 μm. *B*, This diagram illustrates the methodology used in determining the topological distribution of FcγRIIb and CAV-1α in these endothelial cells. In brief, the distance from the abluminal surface (AS) to the luminal surface (LS) of a capillary profile was measured. The distance of a given fluorescence signal (FS) from the abluminal surface was then measured. A relative distance (rD) measurement was then calculated. *C*, The topological distribution of FcγRIIb-positive compartments and caveolae were plotted. The caveolae were concentrated in a narrow zone at or near the abluminal or luminal surface (~80%). FcγRIIb-positive structures, in contrast, were concentrated in the intracellular regions of these cells with ~5% of them at the abluminal surface and another 5% at the luminal surface.

Further, FcγRIIb was not expressed in caveolae. High resolution IFM of villus endothelium double-labeled with anti-FcγRIIb and CAV-1α (the Ab recognizing all caveolae in these cells; T. Takizawa, C. L. Anderson, and J. M. Robinson, manuscript in preparation) showed that CAV-1α was localized to small punctate structures at the luminal and abluminal surfaces consistent with the distribution of caveolae in these cells (26, 27). FcγRIIb, in contrast, was found primarily in intracellular structures interior to the CAV-1α-positive structures (Fig. 3*A*). The two fluorescence signals showed minimal overlap, ~10% (Fig. 2*C*), which likely is accounted for by proximity of separate CAV-1α-positive and FcγRIIb-positive structures; this conclusion is supported by the IEM data below. The topological distribution of FcγRIIb and CAV-1α in placental endothelial cells was assessed. FcγRIIb-positive structures were primarily in the intracellular portion of the cells (~90%) with the luminal and abluminal surfaces each having ~5% (Fig. 3, *B* and *C*). In contrast, CAV-1α-positive structures were primarily present at or near the luminal and abluminal surfaces (~80%) (Fig. 3, *B* and *C*).

Abs to a variety of other marker proteins were tested similarly with double-label IFM. We used Abs to mannose-6-phosphate receptor (late endosome and *trans*-Golgi network marker), transferrin receptor (recycling endosome marker), clathrin (coated pit marker), dynamin II (coated pit marker), Bip/GRP (endoplasmic reticulum marker), p230 (*trans*-Golgi network marker), GM 130 (Golgi marker), cathepsin D (lysosomal matrix marker), CD31 (endothelial plasma membrane marker), and Factor VIII related antigen (endothelial cell-specific Weibel-Palade body marker). No colocalization of FcγRIIb with any of these marker proteins was noted (Fig. 2*C*, and data not shown).

FcγRIIb-positive structures appear very numerous in IFM preparations. The number of FcγRIIb compartments was compared with other compartments present in high number (CAV-1α-positive), relatively high number (EEA 1-, LAMP 1-, and LAMP 2-positive), and relatively low number (GM 130- and p230-positive) in the same endothelial cells. The results support the conclusion that the FcγRIIb-positive compartment is highly abundant in villus placental endothelium (Table II). In another assay, we measured the surface area of endothelium in ultrathin cryosections and found the fluorescence signal for FcγRIIb detection occupied 8% of the cross-sectional space compared with 6% for CAV-1α. Whether the predominance of FcγRIIb is due to differences in absolute number of Ag molecules or Ab avidity awaits further studies.

Distribution of IgG in the placenta

The distribution of IgG in terminal and intermediate villi was determined by IFM using fluorochrome-labeled goat anti-human IgG. IgG was found in punctate structures in the cytoplasm of both the STB and endothelium, and in an amorphous pattern in the ECM (Fig. 4*A*). Quantifying fluorescence intensity of the IgG signal in villi sections, we found the puncta in the apical portion of the STB and endothelium to be equivalent, whereas the fluorescence intensity in the ECM was much brighter, approximately seven

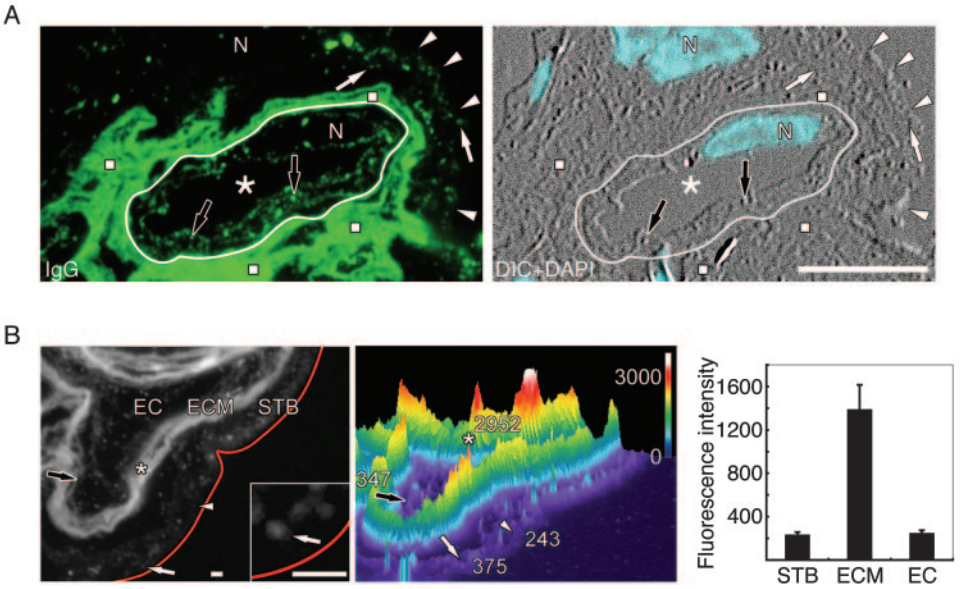

FIGURE 4. The distribution of IgG and its relative concentration in different compartments in the placental terminal villi. *A*, Immunofluorescence localization of IgG in a terminal villus. IgG was localized to vesicular structures in the STB (white arrows), to vesicular structures in the endothelium (black arrow), and to the ECM (white squares). The outer boundary of the endothelial cell is indicated with a white line; the capillary lumen is also indicated (∗). The outer border of the STB is denoted (white arrowheads). Nuclei (N) in the STB and endothelium are indicated. The companion DIC image (*right*) of the section, with DAPI-stained nuclei, shows the morphology of the ultrathin section. The outer boundary of the endothelial cell is indicated with a white line; the capillary lumen is also indicated (∗). Bar, 10 μm. *B*, Fluorescence intensity measurements associated with apical vesicular structures in the STB, vesicular structures in the endothelium (endothelial cell (EC)), and in the ECM were determined following localization of IgG with a fluorochrome-labeled anti-IgG. Fluorescence signal (*left*) is shown from the localization of IgG in an ultrathin cryosection of a terminal villus. A red line indicates the outer boundary of the STB. Two apical vesicles in the STB are indicated (white arrow and arrowhead), also denoted is a vesicle in the endothelium (black arrow) and a region of the ECM (∗). The *inset* shows a higher magnification view (*inset*) of an apical vesicle in the STB (arrow). Bars, 10 μm. Fluorescence intensity profile (*middle*) of the ultrathin cryosection. The fluorescence intensity values of the structures indicated in the micrographs are shown (i.e., white arrow and arrowhead, black arrow, and ∗). Histogram at the *right* summarizes the fluorescence intensity measurements for apical puncta in the STB, puncta in the endothelium, and in the ECM (mean ± SD).

times greater than in the cells (Fig. 4*B*). It is unlikely that this difference was due solely to ultrathin cryosectioning. The average diameter of the FcγRIIb-positive compartment (116 nm; see below) can fill the 70- to 100-nm cryosection. In double-label experiments using anti-human IgG and anti-FcγRIIb, we found ~40% of the FcγRIIb puncta of endothelial cells also positive for IgG, whereas the remaining 60% were devoid of IgG signal (Fig. 2, *B* and *C*). However, most of the compartments that did contain IgG also contained FcγRIIb (~80%) (Fig. 2*D*). The nature of the compartments containing the remaining 20% of the IgG has not been characterized fully. However, at least a portion of this IgG was present in multivesicular bodies and was thus destined for degradation (32) (Fig. 2*E*).

Overlap of IgG and FcγRIIb in the capillary endothelium

The distribution of IgG in villus endothelium was determined by IEM using colloidal gold-tagged immunoprobes. IgG was found at or near the luminal and abluminal plasma membranes of the endothelium and in the ECM. IgG was also found within endothelial cells; of these gold particles within the endothelium virtually all were within 20 nm of a membrane profile (96%, 1000 particles counted) (Fig. 5*A*). These gold particles were associated with small membrane-bounded vesicles (sometimes tubules) (average diameter 116 nm ± 21). IgG appeared to be excluded from tight junctions between adjacent endothelial cells (Fig. 5*A*). Gold particles were not observed to penetrate >37 nm beyond the luminal or abluminal openings of the tight junctions (93 junctions scored); the average length of these tight junctions was 620 nm ± 67.

Double-labeled IEM studies colocalizing IgG and FcγRIIb with colloidal gold particles of two different sizes were conducted (Fig. 5*B*). A total of 205 compartments were scored in the 26 different endothelial cells. We found compartments containing FcγRIIb only (43.9%), both FcγRIIb and IgG (42%), and IgG only (14.1%).

Because some of the structures associated with IgG and FcγRIIb were morphologically similar to caveolae, we tested in double-label IEM experiments whether CAV-1α colocalized with FcγRIIb (Fig. 5*C*). Structures within the same regions of endothelial cells were scored for the localization of CAV-1α, FcγRIIb, and both CAV-1α and FcγRIIb. A total of 218 structures were labeled for CAV-1α only, 217 were labeled for FcγRIIb only, whereas eight were labeled for both markers. This result represents a 3.6% overlap of signal as compared with the 10% overlap observed with IFM (Fig. 2*C*). Taken together, the IFM and IEM data indicate that CAV-1α-positive and FcγRIIb-positive structures are separate from each other. However, because both of these compartments are very abundant in these endothelial cells (Table II), they are often in close proximity; so the low levels of apparent colocalization with both IFM and IEM likely represent mixing of signals from closely opposed structures.

The association of IgG with CAV-1α-positive structures was also examined by double-label IEM (Fig. 5*D*). A total of 131 positively identified caveolae were scored for the presence of IgG. Only 3.5% of these contained particles indicative of IgG localization. There was no distinction between caveolae that were clearly open to the outside of the cell (51%) and those having no apparent connection to the outside (49%); neither contained appreciable IgG.

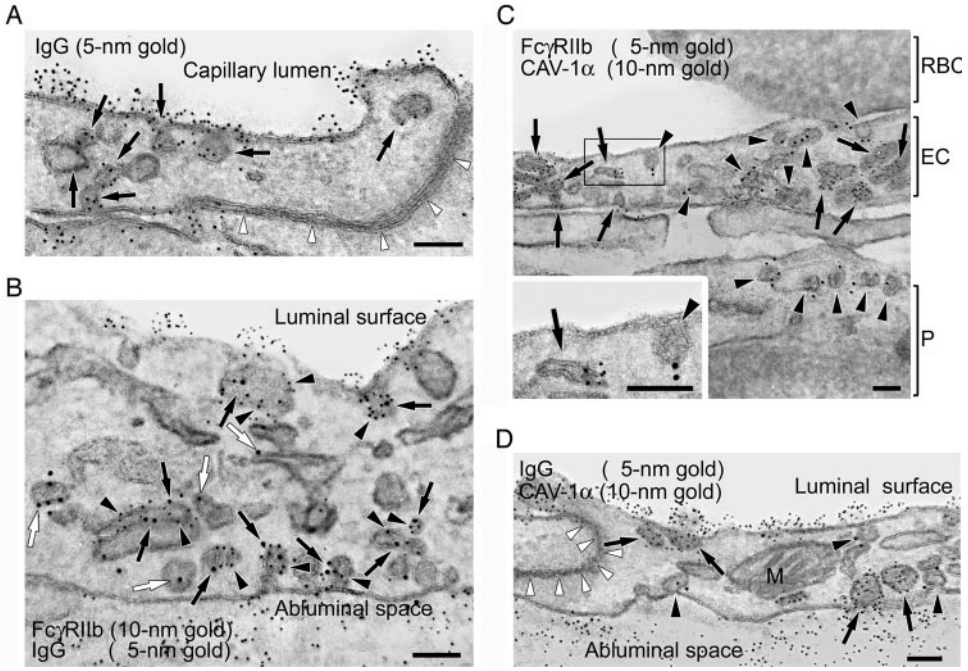

FIGURE 5. Immunoelectron microscopic analysis of ultrathin cryosections of placental endothelial cells in terminal villi. *A*, IgG was found at the apical cell surface, the abluminal space, and in small vesicular and tubular structures (arrows) as demonstrated by 5-nm colloidal gold particles. IgG was not detected in endothelial tight junctions (arrowheads). *B*, The localization of FcγRIIb and IgG using 10- and 5-nm colloidal gold particles, respectively. IgG-containing compartments are indicated (arrowheads). FcγRIIb was localized to small vesicular or tubular structures. There were two types of FcγRIIb-positive compartments: those that contained IgG (black arrows) and those that lacked IgG (white arrows). *C*, The localization of FcγRIIb and CAV-1α in an endothelial cell using 5- and 10-nm colloidal gold, respectively. FcγRIIb was localized to small vesicular and tubular structures (arrows) in the endothelial cell (EC). CAV-1α was localized to structures having the morphological appearance of caveolae (arrowheads) in EC and in a pericyte (P). The boxed area of endothelial cell is shown at a higher magnification (*inset*). *D*, The localization of IgG and CAV-1α using 5- and 10-nm colloidal gold, respectively. IgG was localized to the luminal cell surface, the abluminal space, and intracellular compartments (arrows). CAV-1α was localized to flask-shaped structures with morphological characteristics of caveolae (black arrowheads). IgG was typically absent from CAV-1α-positive structures as it was from the tight junction (white arrowheads). Bars, 100 nm.

Discussion

Our conclusions depend upon the use of an innovative technical feature that deserves comment (29). We used ultrathin cryosections (70- to 100-nm thick in the *z* dimension) not only for EM where they are required but also for IFM where they are seldom used. By way of comparison, resolution typically achieved in the *z* dimension with confocal microscopy of biological material is 500 nm or greater (33, 34). The extraordinary thinness of our sections, approximating the size of the smallest subcellular organelle, minimizes the chance that two organelles lie stacked one on the other in the *z* dimension and thus minimizes false colocalization of FcγRIIb with other organelle markers. This approach thus combines the high sampling efficiency of immunofluorescence, enabling thousands of subcellular structures to be examined with high resolution.

Several conclusions can be drawn from this work. First, we present fresh insight into how IgG might be transferred across the villus endothelium, the second of the two placental cell layers separating a mother's circulation from the fetus. It has long been assumed that IgG moves passively in caveolae that shuttle between the two plasma membranes of the endothelium, the driving force of transport being supplied by FcRn in the STB. However our finding that IgG puncta in endothelium, which must be organelles in transit, are quite separate from CAV puncta would force the conclusion that caveolae do not contain IgG and thus are not involved in the mediation of IgG transfer from mother to fetus. Although heretical, this conclusion may be consistent with fresh observations from CAV-1 knockout mice that lack caveolae. Injection of colloidal gold particles with adsorbed BSA into the circulation of wild-type mice results in accumulation of gold particles in caveolae-like structures; however, gold particles remain in the lumen of blood vessels in the knock out mice (35). This result indicates a role for caveolae in albumin internalization. In contrast, cerebrospinal fluid albumin concentration and the extravascular oncotic pressure were the same in wild type and knockout mice (36). Delivery of albumin to cerebrospinal fluid and normal oncotic pressure are associated with transcytosis of albumin across endothelial cells; these results suggest compensatory transport mechanism independent of caveolae (3). Recent studies indicate that internalization of caveolae is a triggered event (37). Our data would further challenge the notion of caveolae transporting IgG in placental endothelium. Because FcRs have not been found in caveolae of placental endothelium, it may be that IgG does not trigger internalization of caveolae. It should also be noted that the bulk of transport in most vascular beds is in the luminal-to-abluminal direction (3). However, transfer of IgG across the placental endothelium must move in the abluminal-to-luminal direction. Perhaps this difference in directionality provides some explanation for the discord between our results and the generally held view of caveolae-based transcytosis of serum proteins.

We would also conclude from our data that IgG, rather than transiting the villus endothelial cell in caveolae, may be moving to the fetus in association with FcγRIIb. Most of the intracellular IgG (80%) appears to be associated with FcγRIIb, the remaining 20% failing to colocalize with the FcγRIIb compartment. Almost half of the FcγRIIb vesicles contain most of the endothelial IgG (80%)

whereas the remaining FcγRIIb vesicles contain no IgG (see Fig. 2, *C* and *D*). The FcγRIIb organelles appear primarily within the endothelial cells, away from the margins, unlike caveolae, which congregate at or below the plasma membranes. The location of FcγRIIb organelles is compatible with a cargo transferring function across the cell.

Whether FcγRIIb indeed transfers IgG across the endothelium we cannot say from our data. However, there are two details of our study that are worth comment. One is that the ratio of IgG-positive to IgG-negative FcγRIIb organelles, a ratio of roughly 1, would be predicted by a mechanism of one-way FcγRIIb-mediated transport, a mechanism defined by a scenario in which FcγRIIb moves IgG in vesicles from the abluminal side of the endothelium to the luminal side, dumps its cargo at the luminal membrane into the fetal circulation, and then returns in vesicles devoid of IgG to the abluminal side to pick up another load of IgG for another cycle. Alternative explanations, however, are also possible. This particular isoform of the receptor, studies show, is capable of transport. The mouse FcγRIIb2, when expressed by transfection, mediates endocytosis and transcytosis, unlike its companion isoform, FcγRIIb1, which fails to enter endocytic vesicles (7–9). Its low but finite affinity for ligand should not pose an impediment to transport, because many essential functional processes are the result of low affinity interactions (38). Rather, the feature needed by an efficient transporter is dual affinity for ligand. In fact, crystallographic studies of this family of receptors have suggested the possibility that receptor dimers might interact with a single ligand, thus conferring high and low binding affinities for ligand (Refs. 39–41, and our discussion Ref. 4).

Another detail of our study that appears germane to the mechanism of IgG transcytosis is the apparent high concentration of IgG in the villus interstitium between the STB and the endothelial cell. The intensity of IgG-associated fluor appears much brighter (7-fold) than the intensity of intracellular IgG puncta, suggesting the possibility of a concentration gradient established at a high level by FcRn in the interstitium and moving downward across the endothelium toward the fetal circulation. Thus, IgG would move down the concentration gradient perhaps in association with FcγRIIb but without requiring directional and active transport by FcγRIIb. Our data are consistent with the concept of IgG entering the endothelial cells on the abluminal side by a nonclathrin and noncaveolae pathway where IgG encounters FcγRIIb. The FcγRIIb-positive compartment then delivers IgG to the luminal front by a transcytotic process. However, at present we cannot definitively conclude that this is a unique transcytotic pathway or whether it is related to a previously described nonclathrin or noncaveolar pathway.

We are attracted to the notion that FcγRIIb mediates IgG transfer across the endothelium as a resolution to the recently noted paradox that FcRn transports both IgG and albumin, yet albumin cannot easily be shown to be transported like IgG across the placenta in humans (42, 43). The paradox would be resolved if FcγRIIb, binding IgG and not albumin, ferried only IgG and not albumin (44). FcRn of the STB transports both ligands but FcγRIIb2 of the endothelium allows only IgG to pass. We are testing this hypothesis.

We find it noteworthy that the FcγRIIb organelle, despite appearing as the most abundant organelle in the endothelium, cannot be identified with a large battery of common organelle markers. We are tentatively concluding that it is unique. It may be relevant that in preliminary experiments we find FcγRIIb expressed in the endothelium of the vitelline vessels of the mouse yolk sac, suggesting that FcγRIIb2 may be the primordial FcγR in the developing mouse, predating the appearance of fetal IgG and blood cells, serving perhaps to transport maternal IgG to the developing embryo. In such transient germinal tissues it may not be out of the question to find a unique organelle similar to that in human placenta.

Acknowledgments

We thank Heather Richard for technical assistance. We also thank Drs. Shigeki Matsubara and Takeshi Takayama, Jichi Medical School, for technical support. We thank Dr. Fumimaro Takaku, President of Jichi Medical School for encouragement. We are also indebted to Drs. J.-L. Teillaud, J. Frey, D. Mason, and P. Newman for providing Abs.

Disclosures

The authors have no financial conflict of interest.

References

1. Junghans, R. P. 1997. Finally! The Brambell receptor (FcRB). *Immunol. Res.* 16: 29–57.
2. Ghetie, V., and E. S. Ward. 2000. Multiple roles for the major histocompatibility complex class I-related receptor FcRn. *Annu. Rev. Immunol.* 18: 739–766.
3. Tuma, P. L., and A. L. Hubbard. 2003. Transcytosis: crossing cellular barriers. *Physiol. Rev.* 83: 871–932.
4. Lyden, T. W., J. M Robinson, S. Tridandapani, J. L. Teillaud, S. A. Garber, J. M. Osborne, J. Frey, P. Budde, and C. L. Anderson. 2001. The Fc receptor for IgG expressed in the villus endothelium of human placenta is FcγRIIb2. *J. Immunol.* 166: 3882–3889.
5. Callanan, M. B., P. LeBaccon, P. Mossuz, S. Duley, C. Bastard, R. Hamoudi, M. J. Dyer, G. Klobeck, R. Rimokh, J. J. Sotto, and D. Leroux. 2000. The IgG Fc receptor, FcγRIIb, is a target for deregulation by chromosomal translocation in malignant lymphoma. *Proc. Natl. Acad. Sci. USA* 97: 309–314.
6. Tridandapani, S., K. Siefker, J. L. Teillaud, J. E. Carter, M. D. Wewers, and C. L. Anderson. 2002. Regulated expression and inhibitory function of FcγRIIb in human monocytic cells. *J. Biol. Chem.* 277: 5082–5089.
7. Miettinen, H. M., J. K. Rose, and I. Mellman. 1989. Fc receptor isoforms exhibit distinct abilities for coated pit localization as a result of cytoplasmic domain heterogeneity. *Cell* 58: 317–327.
8. Miettinen, H. M., K. Matter, W. Hunziker, J. K. Rose, and I. Mellman. 1992. Fc receptor endocytosis is controlled by a cytoplasmic domain determinant that actively prevents coated pit localization. *J. Cell Biol.* 116: 875–888.
9. Hunziker, W., and I. Mellman. 1989. Expression of macrophage-lymphocyte Fc receptors in Madin-Darby canine kidney cells: polarity and transcytosis differ for isoforms with or without coated pit localization domains. *J. Cell Biol.* 109: 3291–3302.
10. Simister, N. E. 1998. Human placental Fc receptors and the trapping of immune complexes. *Vaccine* 16: 1451–1455.
11. Simister, N. E. 2003. Placental transport of immunoglobulin G. *Vaccine* 21: 3365–3369.
12. Scherer, P. E., Z. Tang, M. Chun, M. Sargiacomo, H. F. Lodish, and M. P. Lisanti. 1995. Caveolin isoforms differ in their N-terminal protein sequence and subcellular distribution: identification and epitope mapping of an isoform-specific monoclonal antibody probe. *J. Biol. Chem.* 270: 16395–16401.
13. Scherer, P. E., R. Y. Lewis, D. Volonte, J. A. Engelman, F. Galbiati, J. Couet, D. S. Kohtz, E. van Donselaar, P. Peters, and M. P. Lisanti. 1997. Cell-type and tissue-specific expression of caveolin-2: caveolins 1 and 2 co-localize and form a stable hetero-oligomeric complex in vivo. *J. Biol. Chem.* 272: 29337–29346.
14. Rappoport, J. Z., S. M. Simon, and A. Benmerah. 2004. Understanding living clathrin-coated pits. *Traffic* 5: 327–337.
15. Mu, F-T., J. M. Callaghan, O. Steele-Mortimer, R. G. Parton, P. L. Campbell, J. McClusky, J. P. Yeo, E. P. Tock, and B. H. Toh. 1995. EEA1, an early endosome-associated protein. *J. Biol. Chem.* 270: 13503–13511.
16. Sanders, S. L., and R. Schekman. 1992. Polypeptide translocation across the endoplasmic reticulum. *J. Biol. Chem.* 267: 13791–13794.
17. Nakamura, N., C. Rabouille, R. Watson, T. Nilsson, N. Hui, P. Slusarewicz, T. E. Kreis, and G. Warren. 1995. Characterization of a *cis*-Golgi matrix protein, GM130. *J. Cell Biol.* 131: 1715–1726.
18. Erlich, R., P. A. Gleeson, P. Campbell, E. Dietzsch, and B. H. Toh. 1996. Molecular characterization of *trans*-Golgi p230. *J. Biol. Chem.* 271: 8328–8337.
19. Conner, G. E. 1992. The role of cathepsin D propeptide in sorting to the lysosome. *J. Biol. Chem.* 267: 21738–21745.
20. Chen, J. W., T. L. Murphy, M. C. Willingham, I. Pastan, and J. T. August. 1985. Identification of two lysosomal membrane glycoproteins. *J. Cell Biol.* 101: 85–95.
21. Dintzis, S. M., V. E. Velculescu, and S. R. Pfeffer. 1994. Receptor extracellular domains may contain trafficking information: studies of the 300-kDa mannose 6-phosphate receptor. *J. Biol. Chem.* 269: 12159–12166.
22. Clague, M. J. 1998. Molecular aspects of the endocytic pathway. *Biochem. J.* 336: 271–282.
23. Newman, P. J., M. C. Berndt, J. Gorski, G. C. White, S. Lyman, C. Paddock, and W. A. Muller. 1990. PECAM-1 (CD31) cloning and relation to adhesion molecules of the immunoglobulin gene superfamily. *Science* 247: 1219–1222.
24. Micklem, K. J., W. P. Stross, A. C. Willis, J. L. Cordell, M. Jones, and D. Y. Mason. 1990. Different isoforms of human FcRII distinguished by SDw32 antibodies. *J. Immunol.* 144: 2295–2303.

25. Sontag, J. M., E. M. Fykse, Y. Ushkaryov, J. P. Liu, P. J. Robinson, and T. C. Südhof. 1994. Differential expression and regulation of multiple dynamins. *J. Biol. Chem.* 269: 4547–4554.
26. Rosenberg, J. B., P. A. Foster, R. J. Kaufman, E. A. Vokac, M. Moussali, P. A. Kroner, and R. R. Montgomery. 1998. Intracellular trafficking of Factor VIII to von Willebrand factor storage granules. *J. Clin. Invest.* 101: 613–624.
27. Robinson, J. M., and D. D. Vandré. 2001. Antigen retrieval in cells and tissues: enhancement with sodium dodecyl sulfate. *Histochem. Cell Biol.* 116: 119–130.
28. Lyden, T. W., C. L. Anderson, and J. M. Robinson. 2002. The endothelium but not the syncytiotrophoblast of human placenta expresses caveolae. *Placenta* 23: 640–652.
29. Takizawa, T., and J. M. Robinson. 2003. Ultrathin cryosections: an important to for immunofluorescence and correlative microscopy. *J. Histochem. Cytochem.* 51: 707–714.
30. Takizawa, T., C. L. Anderson, and J. M. Robinson. 2003. A new method to enhance contrast of ultrathin cryosections for immunoelectron microscopy. *J. Histochem. Cytochem.* 51: 31–39.
31. Cain, T. J., Y. Liu, T. Takizawa, and J. M. Robinson. 1995. Solubilization of glycosyl-phosphatidylinositol-anchored proteins in quiescent and stimulated neutrophils. *Biochim. Biophys. Acta* 1235: 69–78.
32. Mullins, C., and J. S. Bonifacino. 2001. The molecular machinery for lysosome biogenesis. *BioEssays* 23: 333–343.
33. Majlof, L., and P. O. Forsgren. 1993. Confocal microscopy: important considerations for accurate imaging. *Methods Cell Biol.* 38: 79–95.
34. Zucker, R. M., and O. Price. 2001. Evaluation of confocal microscopy system performance. *Cytometry* 44: 273–294.
35. Schubert, W., P. G. Frank, B. Razani, D. S. Park, C. W. Chow, and M. P. Lisanti. 2001. Caveolae-deficient endothelial cells show defects in the uptake and transport of albumin in vivo. *J. Biol. Chem.* 276: 48619–48622.
36. Drab, M., P. Verkade, M. Elger, M. Kasper, M. Lohn, B. Lauterbach, J. Menne, C. Lindshau, F. Mende, F. C. Luft, et al. 2001. Loss of caveolae, vascular dysfunction, and pulmonary defects in caveolin-1 gene-disrupted mice. *Science* 293: 2449–2452.
37. Pelkmans, L., and A. Helenius. 2002. Endocytosis via caveolae. *Traffic* 3: 311–320.
38. Maenaka, K., P. A. van der Merwe, D. I. Stuart, and P. Sondermann. 2001. The human low affinity Fcγ receptors IIa, IIb, and III bind IgG with fast kinetics and distinct thermodynamic properties. *J. Biol. Chem.* 276: 44898–44904.
39. Sondermann, P., R. Huber, and U. Jacob. 1999. Crystal structure of the soluble form of the human FcγRIIb: a new member of the immunoglobulin superfamily at 1.7 Å resolution. *EMBO J.* 18: 1095–1103.
40. Sondermann, P., U. Jacob, C. Kutscher, and J. Frey. 1999. Characterization and crystallization of soluble human Fcγ receptor II (CD32) isoforms produced in insect cells. *Biochemistry* 38: 8469–8477.
41. Maxwell, K. F., M. S. Powell, M. D. Hulett, P. A. Barton, I. F. McKenzie, T. P. Garrett, and P. M. Hogarth. 1999. Crystal structure of the human leukocyte Fc receptor, FcRIIa. *Nature Struct. Biol.* 6: 437–442.
42. Dancis, J., J. Lind, M. Oratz, J. Smolens, and P. Vara. 1961. Placental transfer of proteins in human gestation. *Am. J. Obstet. Gynecol.* 82: 167–171.
43. Gitlin, D., J. Kumate, M. Urrusti, and C. Morales. 1964. The selectivity of the human placenta in the transfer of plasma proteins from mother to fetus. *J. Clin. Invest.* 43: 1938–1951.
44. Chaudhury, C., S. Mehnaz, J. M. Robinson, W. L. Hayton, D. K. Pearl, D. C. Roopenian, and C. L. Anderson. 2003. The MHC-related Fc receptor for IgG (FcRn) binds albumin and prolongs its lifespan. *J. Exp. Med.* 197: 315–322.